# Optical Fiber Devices and Their Applications

**Yutaka SASAKI**
**Faculty of Engineering**
**Ibaraki University**
**4-12-1, Nakanarusawa-cho, Hitachi, Ibaraki 316-8511, Japan**

*ABSTRACT:* - Recent progress in research on optical fiber devices, especially optical fiber couplers and optical fiber grating couplers, by a new fabrication method, that is, a $CO_2$ laser irradiation method is reviewed. Furthermore, applications of optical fiber grating couplers are also described.

*Key-words:* - Optical Fiber Device, Optical Fiber Coupler, Optical Fiber Grating Coupler

## 1 Introduction

For the lowest insertion loss and simplest implementation device, which are effective for access networks, an all-fiber solution is preferred. By the way, numerous optical fiber devices have been proposed and used as optical multi/ demultiplexers and optical filters for optical transmissions. Optical fiber couplers (FCs) by fusion methods[1] and optical fiber gratings (FGs)[2],[3] have been already applied as fundamental devices, and the devices combined with the FCs[4],[5] and the FGs such as optical fiber grating couplers (FGCs)[6],[7],[8] are proposed as new devices offering functions of optical multi/demultiplexing, wavelength selectivity and so on.

The FCs are commercially available, but now they need precisely controlled fabrication conditions for compact FCs with small-size. They are also required to take short time to produce because of productivity and to be produced without contaminations from heat sources because of reliability.

The FGCs, whose four-ports operate effectively for optical multi/demultiplexing and wavelength selectivity, are desired to be all-fiber devices for low-insertion loss, simple implementation and low-cost.

## 2 FCs by fusion methods

Fabrications of FCs by fusion methods are now carried out by the flame method using micro-burners and the thermal heating method using micro-heaters. These methods have demerits on precise control of design parameters such as taper shapes of the FCs. They take much time to produce, for example, several minutes in melting a section of silica fiber and are followed by contaminations from the flames or the micro-heaters. So, laser irradiation (LI) methods by a $CO_2$ laser as heat source in the fusion methods[4],[5],[9] were recently proposed to overcome these drawbacks.

### 2.1 Laser irradiation (LI) method

LI methods[4],[5],[9] have four merits of small heating spot, measurable/controllable LI power, clean heat source, and short time fusion of a section of silica fiber. The use of a stabilized $CO_2$ laser can focus large amounts of measurable and controllable power very quickly to a small area, and it is also clean and insensitive to environmental disturbances.

One of typical LI method[4],[5] is shown in Fig. 1, which uses a $CO_2$ laser with CW or pulse operations, providing the power of heating the fiber. The laser is focused with two ZeSe cylindrical lenses, whose spot is varied by moving the lens positions. A He-Ne laser guide is used to adjust the LI position on the fiber. The LI power is irradiated to be constant or temporally variable under fixed LI spot being circle or ellipse. Other technique using a $CO_2$ laser[9] is also reported, in which the small LI spot over the fiber is positioned and then scanned along the fiber with a galvanometer mirror.

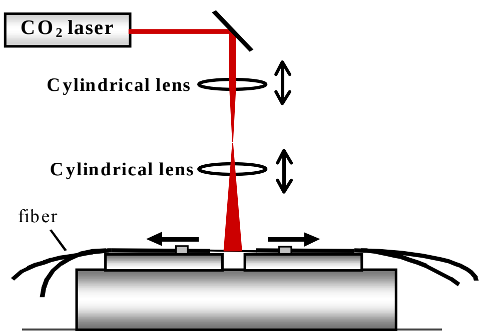


Fig. 1 FC fabrication setup

## 2.2 Compact FC with small-size

An analysis model of a compact FC with small-size is shown in Fig. 2, where $z$ is the distance from the FC center and the FC taper diameter $c(z)$ is defined as the distance between the outside points in the cross section of the two fibers. Here, $c_{min}= c(0)$, $c_0 = 4b$ where $2b$ is the original fiber diameter and $d(z)$ is the distance between the fiber core centers. Furthermore, the FC taper length $L_c$ is defined as the distance between the cross sections in which $c(z)=0.9 \times c_0$. Important parameters in the FC design are fusion ratio $\eta$ and elongation ratio $\tau$. They are defined as $\eta = d(0)/2b$ and $\tau = c_{min}/c_0$.

A small-sized 3 dB FC with $L_c$ of 11.3 mm was fabricated by the LI method. In the process of fabrication, first, the normal LI method, irradiated with constant laser power and followed by elongation, was carried out. Second, LI without elongation was operated. Last, the LI method with the intermittent LI having the same laser power, followed by elongation simultaneously, was carried out. The excess loss of 0.3 dB is gained with 0.63 of $\eta$ and 0.40 of $\tau$. The taper shape of the fabricated FC is approximated SIN$^2$ type[10].

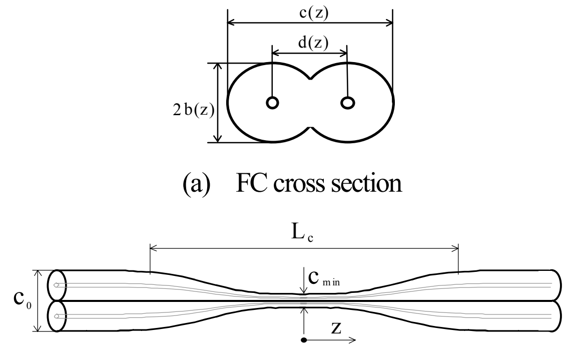


(a) FC cross section

(b) Side view of FC

Fig. 2 Analysis model of FC

# 3 FGC

The designs based on grating written in coupling region of polished FCs[11],[12] have been demonstrated, but they do not represented a satisfactory solution to producing compact, stable, and low-cost components.

An FGC have been newly proposed[6] and fabricated [7],[8]. It is combined with the FC by fusion methods and the Bragg gratings written in the coupling region, that is, the FC taper region. This device offers low-insertion loss, simple implementation, and low-cost.

## 3.1 Configuration and operation of FGC

Fig. 3 shows a configuration of the FGC, in which the Bragg grating is written in the taper region of the FC having "one cross path" around the Bragg wavelength $\lambda_B$. The grating with length of $L_g$ is written by two-beam holographic method using an Ar-SHG laser as coherent UV light and the light at $\lambda_B$ is dropped in port 2.

Drop efficiency ($DE$) and through efficiency ($TE$) are shown as $DE=P_2/P_1$ and $TE=P_4/P_1$, respectively, using $P_1$ of the launched power in port 1, $P_2$ of the dropped power in port 2 and $P_4$ of the transmitted power in port 4.

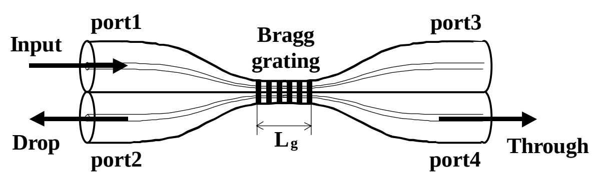


Fig. 3 Optical fiber grating coupler (FGC)

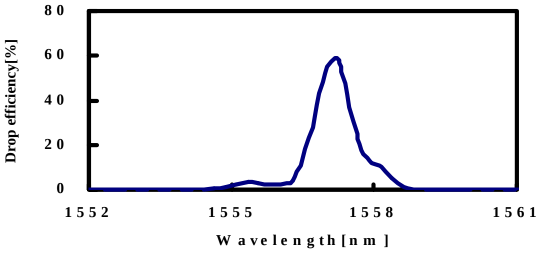


(a) Drop efficiency (*DE* )

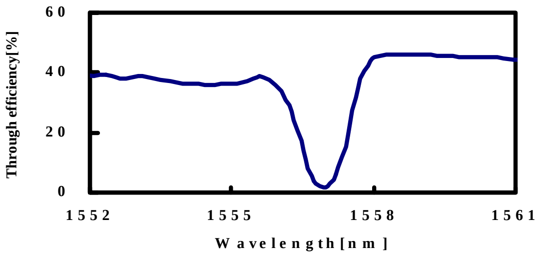


(b) Through efficiency (*TE* )

Fig. 4 Spectral characteristics of FGC

### 3.2 Spectral characteristics of FGC

The spectral characteristics of the fabricated FGC are shown in Fig. 4. It is found from Fig. 4 (a) that *DE* is 60 % at $\lambda_B$ = 1557 nm and the spectral width is about 0.8 nm. From Fig. 4 (b), *TE* is found to be about 1.7 % at $\lambda_B$. Here, the FC made of conventional single-mode fiber was produced by the LI method using a $CO_2$ laser. Furthermore, it was then hydrogen-loaded at 20 MPa for two weeks. $L_c$ and $L_g$ were 9 mm and 6 mm, respectively.

## 4 Applications of FGCs

We proposed applications of FGCs for noise reduction, gain monitoring, add-drop multiplexing and all-optical switching. FGC applications for noise reduction and gain monitoring are concerned with signal amplifications by Er-doped optical fiber amplifiers (EDFAs) in wavelength division multiplexing (WDM) transmissions. The amplified spontaneous emission (ASE) noise generates by using EDFAs. So, noise reduction improves optical signal to noise ratios (OSNRs) and gain monitoring contributes to signal stabilizations. And those of add-drop multiplexing and all-optical switching are concerned with signal switching in WDM fiber routings.

### 4.1 ASE noise reduction in EDFAs

A configuration for OSNR improvement by reducing ASE noise using a cascaded FGC filter in EDFA repeaters for WDM signals was proposed[14]. A configuration and basic operations for a single wavelength are described. The operation for WDM signals is also described in detail.

#### 4.1.1 ASE noise reduction by using cascaded FGCs

Fig. 5 shows a configuration for OSNR improvement by reducing ASE noise in an EDFA repeater using the cascaded FGCs for WDM signals. Each of the FGCs has a Bragg grating at a different wavelength with each other, written "one cross path" FC. Writing the grating with proper offset length in the taper region of the FC, the signal at the Bragg wavelength can be dropped to port 2 of the FGC when WDM signals are launched into port 1. Other signals apart from the Bragg wavelength are transmitted to port 4 of the FGC.

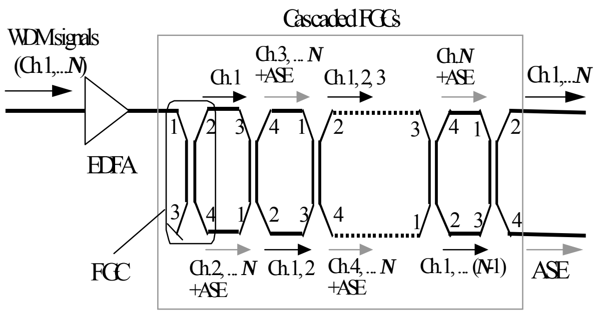


Fig. 5 Configuration of cascaded FGCs

The operation of cascaded *N* FGCs for WDM signals with *N* channels is shown in Fig. 5. In the figure, the signal streams, which are reduced the ASE noise, are indicated as black arrows, and the main ASE noise streams, which follow the signals, are indicated as gray arrows. The Bragg wavelength of each FGC corresponds to the wavelength of each WDM signal. The signal at the Bragg wavelength is dropped to port 2 of each FGC and launched into port 3 of the next FGC. Thus, after the *N* th FGC, the main ASE noise is separated from the WDM signals and transmitted to port 4 of the *N* th FGC, and the WDM signals are transmitted to port 2.

### 4.1.2 Noise reduction characteristics

Fig. 6 shows an experimental setup to estimate basic characteristics of ASE noise reduction for single wavelength. The *DE* of the fabricated FGC is 45 % (–3.5 dB) at $\lambda_B$ of 1553.3 nm. This value is large enough in spite of using a conventional single-mode fiber with pure silica cladding. The *DE* spectrum (FWHM) is 1 nm. In our setup, the FGC is operated as a WDM-FC for pumping laser with 980 nm wavelength. The extinction ratio of the output power from port 1 to from port 2 is 18 dB when the pumping laser is launched from port 3. The amplified signal spectra were measured using an optical spectrum analyzer (OSA) with 0.007 nm resolution.

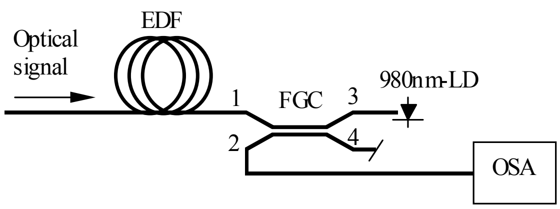


Fig.6 Experimental setup

Fig. 7 shows amplified signal spectra. The black line shows an amplified spectrum in the setup of Fig. 6. The peak power of input signal was –14.9 dB. A gain of the setup was 5.3 dB taking account of FGC loss as the peak power of the amplified signal was –9.2 dB. For confirmation of the FGC effect, an amplified signal spectrum using usual backward pump (without FGC) EDFA with 5.3 dB gain was measured (gray line). It is shown that ASE noise except signal wavelength can be reduced using the FGC. Since 7 dB ASE noise reduction was obtained in the wavelength range of 1525-1565 nm, it is confirmed that OSNR can be improved by reducing the ASE noise using the FGC with an EDFA.

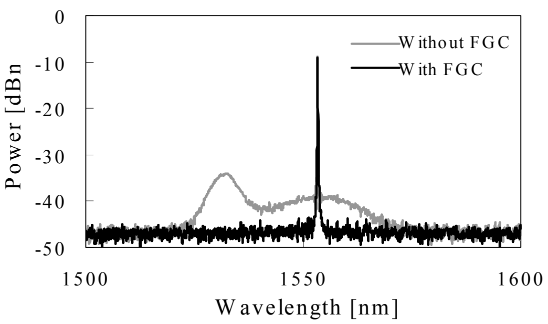


Fig. 7 Amplified signal spectra

### 4.2 Gain monitoring of EDFAs

Since EDFAs have been widely researched and developed, EDFAs are now commercially available and used for actual optical transmission systems with long distance. Recently, there are more requirements for EDFAs than ever as they are also used for WDM optical transmission systems. The requirements are flat gain spectrum and stabilized gain [14].

So, we proposed an EDFA gain monitoring method by detecting ASE noise level using an FGC in WDM transmission systems, as applications of FGCs.

### 4.2.1 EDFA gain monitoring by using FGCs

Fig. 8 shows a configuration for EDFA gain monitoring by ASE level detection using an FGC. The FGC consists of "one cross path" FC. When WDM signals are launched into port 1, the signal at the Bragg wavelength $\lambda_B$ can be dropped to port 2 and other signals transmit to port 4.

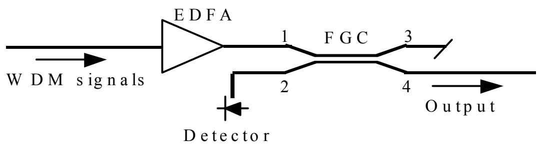


Fig. 8 EDFA gain monitoring using FGC.

In the configuration, the Bragg wavelength at which the ASE power is dropped is apart from the signal one. As the number of WDM channels increases, the EDFA gain increases. So, the dropped ASE power, depending on the EDFA gain, also increases. As a result, the number of signal-stopped channels is found to be detected by using the proposed configuration.

### 4.2..2 Gain monitoring characteristics

The 3-channel WDM signals were multiplexed by a star-coupler and launched into the EDFA through an optical attenuator. The signal wavelengths of 1552.0nm, 1553.2nm and 1554.4nm were used. The incident peak powers of WDM signals with –30 dBm were amplified with 20 dB gain. $\lambda_B$ of the used FGC was, and the *DE* at

$\lambda_B$ of 1555.9nm was 42% (–3.8 dB). The EDFA was used an usual silica-based EDF and backward pumped at 1480nm.

Fig. 9 shows the dropped ASE power vs. the number of signal-stopped channels. The dropped ASE power was estimated by integration of the spectrum from 1545nm to 1565nm. It was confirmed from this figure that the number of signal-stopped channels is detected by monitoring the dropped ASE power.

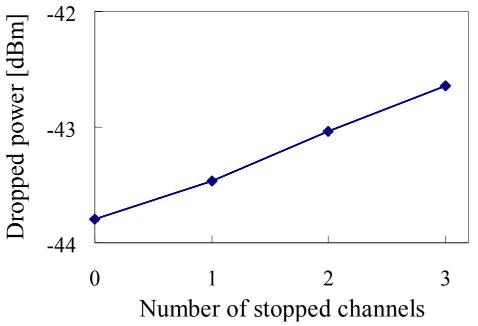


Fig.9 Dropped ASE power for number of signal-stopped channels.

## 4.3 Add-drop multiplexing

ADMs are key devices to construct WDM transmission systems, especially optical fiber routing WDM systems.

### 4.3.1 Add-drop multiplexing for WDM transmissions

We proposed two fundamental ADMs[14], which are a single and a pair of ADMs, shown in Fig. 10 (a) and (b).

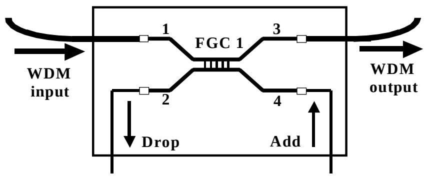


(a) Configuration of a single FGC

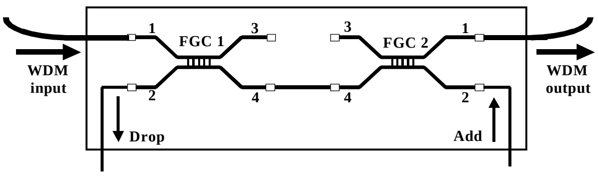


(b) Configuration of a pair of FGCs

Fig.10 Fundamental ADMs

### 4.3.2 Add-drop multiplexing characteristics

Fig. 11 (a) and (b) show the results using a single FGC and a pair of FGCs, respectively. We can find the difference between drop efficiency and add efficiency in Fig.11 (a). The difference occurs by the immature fabrication techniques. In Fig.11 (b), we can find to already gain a pair of FGCs which has the uniformly assembled characteristics.

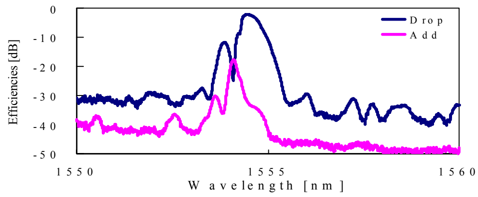


(a) ADM of a single FGC

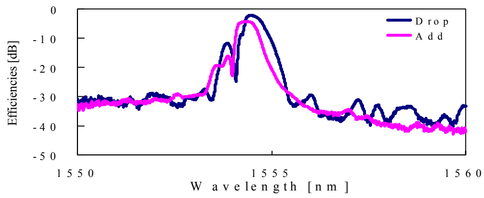


(b) ADM of a pair of FGCs

Fig. 11 Drop and add efficiencies for wavelength.

Furthermore, we proposed a modified ADM which is composed of a fundamental ADM shown in Fig. 10 (b), an EDF and a pumping laser[13]. The ADM has the ability of signal amplification and OSNR improvement. Compared with the case without the EDF and the pumping laser, gain of 8 dB is obtained.

## 4. 4 All-optical switching based on Kerr nonlinearity

Future optical fiber transmission systems will be strongly required to have much capacity and high-speed response. Especially, high-speed and high-stable optical cross connect systems (OXCSs) will be demanded for core, metro and access optical networks, where all-optical sytems are expected to exert speedy and stable functions on those optical networks.

So, our proposal for applications of FGCs is an all-optical switching using Kerr nonlinearity in FGCs.

#### 4.4.1 All-optical switching by using FGCs

Proposed all-optical switching using Kerr nonlinearity in an FGC is shown in Fig. 12. The signal power is coupled by means of a WDM-FC to a high pump power and those powers are launched into port 1 of the FGC. The intense pump induces a nonlinear variation of the refractive index that shifts the DE-spectrum of the signal wavelength towards longer wavelength. Therefore, if $\lambda_B$ of the FGC is set in the bandwidth of the DE-spectrum, the signal is dropped to port 2 (or transmits through to port 4) when the pump is copropagating with the signal (or not). The origin of the all-optical switching is Kerr nonlinearity.

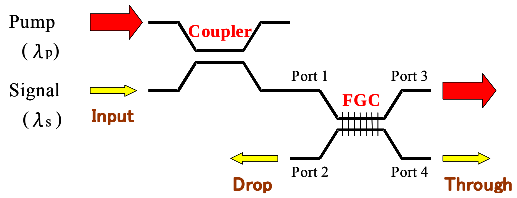


Fig. 12 Proposed all-optical switching.

#### 4.4.2 Fundamental operations of all-optical switching

The experimental results are shown in Fig. 13. A high power Ti-sapphire pulse laser emitting at 780 nm was used. The pump pulsewidth is between 1.2-1.5ps, depending on the energy output level and the pulse rate is 80 MHz. The grating length of the FGC was 6 mm and the index profile was Gaussian apodized.

The dropped signal power was measured by the lock-in amplifier after being detected with an photodiode. The lock-in amplifier output, that is, the dropped signal power decreases as the pump peak power increases. As a result, it was confirmed that the all-optical switching based on Kerr nonlinearity was observed.

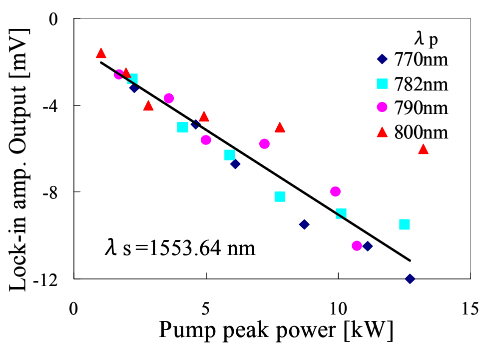


Fig13 Lock-in amp. output vs. pump peak power.

# 5 Summary

LI method by a $CO_2$ laser for FC fabrication was presented.

FGCs were proposed and measured the spectra, and were confirmed to drop the signal at the Bragg wavelength. Furthermore, we proposed and confirmed experimentally applications of FGCs for noise reduction, gain monitoring, add-drop multiplexing and all-optical switching.

In the near future, these all-fiber devices will realize low-loss and low-cost fiber routing WDM systems.

*References:*


[1] B. S. Kawasaki, et al., *Opt. Lett.*,Vol.6, 1981, p.327.

[2] K. O. Hill and G. Meltz, *J. Lightwave Technol.*, Vol.15, No.8, 1997, pp.1263-1276.

[3] T. Erdogan, *J. Lightwave Technol.*, Vol.15, No.8, 1997, pp.1277- 1294.

[4] H. Yokota, E. Sugai, Y. Kashima and Y. Sasaki, *OFS-11*, Conf. Proc., Th3-19, pp.494-497, 1996.

[5] H. Yokota, E. Sugai and Y. Sasaki, *Opt. Rev.*, Vol.4, No.1A, 1997, pp.104-107.

[6] H. Yokota, T. Hasegawa, E. Sugai and Y. Sasaki, *OECC'97*, Tech. Dig., 9D1-5, pp.214-215, 1997.

[7] F. Bakhti, P. Sansonetti, C. Sinet, L. Martineau, S. Lacroix, X. Daxhelet and F. Gonthier, *Electron. Lett.*, Vol.33, No.9, 1997, pp.803-804.

[8] H. Yokota, T. Hasegawa, Y. Satoda, E. Sugai and Y. Sasaki, *Opt. Rev.*, Vol.6, No.3, 1999, pp.173-179.

[9] G. Kakarantzas, et al., *CLEO/Pasific Rim'99*, Tech. Dig., WB1, p.127, 1999.

[10] Y. Sasaki, Proc. *22nd Meet. on Lightwave Sens. Technol.*, pp.35-42, 1998.

[11] J. L. Archambault, et al., *OFC'94* , Tech. Dig., TuL5, p.51, 1994.

[12] I. Baumann, J. Seifert, W. Nowak and M. Sauer, *IEEE Photon. Technol. Lett.*, Vol.8, No.10, 1996, pp.1331-1333.

[13] H. Yokota, Y. Satoda, J. Igarashi, S. Ohuchi and Y. Sasaki, Proc. *APCC/OECC'99*, Vol.1, pp.477-478, 1999.

[14] H. Yokota, K. Kamoto, J. Igarashi, N. Mouri and Y. Sasaki, *OFC2001*, Tech. Dig., WI3, 2001.